



Fraunhofer Institut
Techno- und
Wirtschaftsmathematik

M. Günther, A. Klar, T. Materne, R. Wegener

Multivalued fundamental diagrams and stop and go waves for continuum traffic equations

© Fraunhofer-Institut für Techno- und
Wirtschaftsmathematik ITWM 2002

ISSN 1434-9973

Bericht 35 (2002)

Alle Rechte vorbehalten. Ohne ausdrückliche, schriftliche Genehmigung des Herausgebers ist es nicht gestattet, das Buch oder Teile daraus in irgendeiner Form durch Fotokopie, Mikrofilm oder andere Verfahren zu reproduzieren oder in eine für Maschinen, insbesondere Datenverarbeitungsanlagen, verwendbare Sprache zu übertragen. Dasselbe gilt für das Recht der öffentlichen Wiedergabe.

Warennamen werden ohne Gewährleistung der freien Verwendbarkeit benutzt.

Die Veröffentlichungen in der Berichtreihe des Fraunhofer ITWM können bezogen werden über:

Fraunhofer-Institut für Techno- und
Wirtschaftsmathematik ITWM
Gottlieb-Daimler-Straße, Geb. 49

67663 Kaiserslautern

Telefon: +49 (0) 6 31/2 05-32 42

Telefax: +49 (0) 6 31/2 05-41 39

E-Mail: info@itwm.fhg.de

Internet: www.itwm.fhg.de

Vorwort

Das Tätigkeitsfeld des Fraunhofer Instituts für Techno- und Wirtschaftsmathematik ITWM umfasst anwendungsnahe Grundlagenforschung, angewandte Forschung sowie Beratung und kundenspezifische Lösungen auf allen Gebieten, die für Techno- und Wirtschaftsmathematik bedeutsam sind.

In der Reihe »Berichte des Fraunhofer ITWM« soll die Arbeit des Instituts kontinuierlich einer interessierten Öffentlichkeit in Industrie, Wirtschaft und Wissenschaft vorgestellt werden. Durch die enge Verzahnung mit dem Fachbereich Mathematik der Universität Kaiserslautern sowie durch zahlreiche Kooperationen mit internationalen Institutionen und Hochschulen in den Bereichen Ausbildung und Forschung ist ein großes Potenzial für Forschungsberichte vorhanden. In die Berichtreihe sollen sowohl hervorragende Diplom- und Projektarbeiten und Dissertationen als auch Forschungsberichte der Institutsmitarbeiter und Institutsgäste zu aktuellen Fragen der Techno- und Wirtschaftsmathematik aufgenommen werden.

Darüberhinaus bietet die Reihe ein Forum für die Berichterstattung über die zahlreichen Kooperationsprojekte des Instituts mit Partnern aus Industrie und Wirtschaft.

Berichterstattung heißt hier Dokumentation darüber, wie aktuelle Ergebnisse aus mathematischer Forschungs- und Entwicklungsarbeit in industrielle Anwendungen und Softwareprodukte transferiert werden, und wie umgekehrt Probleme der Praxis neue interessante mathematische Fragestellungen generieren.



Prof. Dr. Dieter Prätzel-Wolters
Institutsleiter

Kaiserslautern, im Juni 2001

Multivalued fundamental diagrams and stop and go waves for continuum traffic flow equations

Marco Günther* Axel Klar† Thorsten Materne‡
Raimund Wegener§

February 27, 2002

Abstract

In the present paper a kinetic model for vehicular traffic leading to multivalued fundamental diagrams is developed and investigated in detail. For this model phase transitions can appear depending on the local density and velocity of the flow. A derivation of associated macroscopic traffic flow equations from the kinetic equation is given. Moreover, numerical experiments show the appearance of stop and go waves for highway traffic with a bottleneck.

keywords traffic flow, macroscopic equations, kinetic derivation, multivalued fundamental diagram, stop and go waves, phase transitions

AMS 76P05, 90B20, 60K15

1 Introduction

Classical models for vehicular traffic consider the continuity equation for the density ρ closing the equation by an equilibrium assumption on the mean velocity u , that means approximating u by an equilibrium value $u^e(\rho)$, [19]. The function $u^e(\rho)$ is the so called fundamental diagram. An additional momentum equation for u has been introduced by Payne and Whitham in [17, 19] in analogy to fluid dynamics. Daganzo [3] has pointed out inconsistencies, like wrong way

*Institut für Techno- und Wirtschaftsmathematik (ITWM), 67663 Kaiserslautern, Germany, (guenther@itwm.fhg.de).

†FB Mathematik, TU Darmstadt, 64289 Darmstadt, Germany, (klar@mathematik.tu-darmstadt.de).

‡FB Mathematik, TU Darmstadt, 64289 Darmstadt, Germany, (materne@mathematik.tu-darmstadt.de).

§Institut für Techno- und Wirtschaftsmathematik (ITWM), 67663 Kaiserslautern, Germany, (wegener@itwm.fhg.de).

traffic, of models such as the Payne-Whitham model in certain situations. The inconsistencies are resolved by the introduction of a new macroscopic model by Aw and Rascle [2]. For a mathematical discussion see [1] or Greenberg [4]. Another basic problem of macroscopic traffic flow equations has been described by Kerner [8, 9, 10]. The observations there suggest a more complicated dependence of the homogeneous steady speed states on density: the states are not given by a uniquely defined function $u = u^e(\rho)$ as used in the above models, but cover a whole range in the density-flow diagram.

Kinetic equations for vehicular traffic can be found, for example, in [18, 16, 15, 11]. Procedures to derive macroscopic traffic equations including the Aw/Rascle model from underlying kinetic models have been performed in different ways by several authors, see, for example, [6] and [13]. These procedures are developed in analogy to the transition from the kinetic theory of gases to continuum gas dynamics. In the present paper a kinetic model is developed allowing for multiple stationary solutions. This leads to multivalued fundamental diagrams. Different steady speed states can appear for fixed density. They may be interpreted as traffic jams or synchronized traffic respectively, compare [10]. We refer to Nelson/Sopasakis [14] for investigations on this point for the Prigogine model and to [5] for investigations on a simplified macroscopic model. Finally, the macroscopic equations derived from the kinetic model exhibit the desired features like stop and go behaviour.

The paper is arranged in the following way: In Section 2 the kinetic model is presented, reduced to a cumulative description of the highway. In Section 3 the stationary distributions of the kinetic model are investigated and the multivalued fundamental diagrams are determined. Section 4 contains the derivation of macroscopic models. Each section is concluded by the discussion of an example. Finally, in Section 5 numerical results are given showing the density-velocity relation and the different homogeneous stationary states which appear in the model. Moreover, a nonhomogeneous traffic flow situation with a bottleneck is investigated, showing the appearance of stop and go waves.

2 The Kinetic Model

The kinetic model developed here is based on the work in [12] and describes highway traffic in a cumulative way averaging over all lanes.

2.1 Preliminaries

The basic quantity in a kinetic approach is the single car distribution $f(x, v)$ describing the density of cars at x with velocity v . Here and in the following we do not write explicitly the time dependence. The total density ρ on the highway is defined by

$$\rho(x) = \int_0^w f(x, v) dv,$$

where w denotes the maximal velocity. Let $F(x, v)$ denote the probability distribution in v of cars at x , i.e. $f(x, v) = \rho(x)F(x, v)$. The mean velocity is

$$u(x) = \int_0^w vF(x, v)dv.$$

An important role is played by the distribution $f^{(2)}(x, v, h, v_+)$ of pairs of cars being at the spatial point x with velocity v and leading cars at $x + h$ with velocity v_+ . This distribution function has to be approximated by the one-vehicle distribution function $f(x, v)$. We use the chaos assumption

$$f^{(2)}(x, v, h, v_+) = q(h, v; \rho, u) f(x, v) F(x + h, v_+),$$

compare Nelson [15]. For a vehicle with velocity v the function $q(h, v; \rho, u)$ denotes the distribution of leading vehicles with distance h under the assumption that the velocities of the vehicles are distributed according to the distribution function f .

Moreover, we introduce the following thresholds for braking (H_B) and acceleration (H_A):

$$H_X(v) = H_0 + vT_X, \quad X = B, A.$$

$T_B = T_B(\rho, u)$ and $T_A = T_A(\rho, u)$ with $T_B < T_A$ are reaction times which may depend on ρ and u . H_0 denotes the minimal distance between the vehicles. We write $H_X = H_X(v) = H_X(v; \rho, u)$. From a microscopic point of view drivers will brake, once the distance between the driver and its leading car is becoming smaller than a threshold H_B and will accelerate, once this distance is becoming larger than H_A . Otherwise the cars will not change the velocities. Velocities are changed instantaneously once acceleration or braking lines are reached. Models including acceleration of the cars can be developed as well, see [7] for an example.

We assume that drivers drive with different behaviour, i.e. with different T_B , allowing for different distances to their leading cars. So called synchronized traffic is associated to smaller T_B and thus smaller distances. This leads to higher velocities at a fixed density. Traffic which is not synchronized is associated to larger T_B and thus to lower speeds at the above density. A special choice of $T_B = T_B(\rho, u)$ is given in the last section.

The distribution of leading vehicles $q(h, v; \rho, u)$ is prescribed a priori. The main properties, which $q(h, v; \rho, u)$ has to fulfill are positivity,

$$\int_0^\infty q(h, v; \rho, u)dh = 1,$$

and

$$\int_0^w \int_0^\infty hq(h, v; \rho, u)dh F(v)dv = \frac{1}{\rho}. \quad (1)$$

Equation (1) means that the average headway of the cars is $1/\rho$. The leading vehicles are assumed to be distributed in an uncorrelated way with a minimal distance H_B from the car under consideration, see Nelson [15]:

$$q(h, v; \rho, u) = \tilde{\rho} e^{-\tilde{\rho}(h-H_B(v))} \chi_{[H_B(v), \infty)}(h).$$

The reduced density $\tilde{\rho}$ has to be defined in such a way, that (1) is fulfilled. One obtains

$$\tilde{\rho} = \frac{\rho}{1 - \rho \int_0^w H_B(v) F(v) dv} = \frac{\rho}{1 - \rho H_B(u; \rho, u)}$$

Remark: *The reduced density $\tilde{\rho}$ must be positive, i.e.*

$$1 - \rho H_B(u; \rho, u) = 1 - \rho(H_0 + uT_B(\rho, u)) > 0$$

This defines a range of admissible values in the (ρ, u) -plane.

The probability P_{ov} for overtaking or lane changing and the corresponding probability $P_B = 1 - P_{ov}$ for braking are determined from microscopic considerations. A car overtakes, if there is sufficient space on the new lane, i.e. if the cars on the new lane have at least a distance $H_B(v)$ from the changing car. Averaging over the distribution function yields

$$P_{ov}(v; \rho, u) = \rho \int_0^w \int_0^w \int_{H_B(v)+H_B(v')}^\infty \int_h^\infty q(h', \tilde{v}; \rho, u) dh' dh F(\tilde{v}) d\tilde{v} F(v') dv'. \quad (2)$$

2.2 The evolution equation

The kinetic model is given by the following evolution equation for the distribution function f :

$$\begin{aligned} \partial_t f + v \partial_x f &= \hat{C}^+(f) \\ &= (\hat{G}_B^+ - \hat{L}_B^+)(f) + (\hat{G}_A^+ - \hat{L}_A^+)(f) + (\hat{G}_S - \hat{L}_S)(f). \end{aligned} \quad (3)$$

\hat{G}_B^+, \hat{L}_B^+ denote the gain and loss terms due to braking and \hat{G}_A^+, \hat{L}_A^+ those due to acceleration interactions. \hat{G}_S and \hat{L}_S are terms describing a random behaviour of the drivers. They are stated in the following:

For the *Braking-Interaction* one obtains the gain term

$$\begin{aligned} \hat{G}_B^+(f) &= \int \int_{\hat{v} > \hat{v}_+} |\hat{v} - \hat{v}_+| q(H_B(\hat{v}), \hat{v}; \rho, u) P_B(\hat{v}; \rho, u) \\ &\quad \sigma_B(v; \hat{v}, \hat{v}_+) f(x, \hat{v}) F(x + H_B(\hat{v}), \hat{v}_+) d\hat{v} d\hat{v}_+ \end{aligned}$$

with the distribution σ_B of new velocities v after the interaction. The loss term is given by

$$\begin{aligned} \hat{L}_B^+(f) &= \int_{\hat{v}_+ < v} |v - \hat{v}_+| q(H_B(v), v; \rho, u) P_B(v; \rho, u) \\ &\quad f(x, v) F(x + H_B(v), \hat{v}_+) d\hat{v}_+. \end{aligned}$$

In other words, the driver is braking if he is not changing to the left lane for overtaking. Reaching the braking line the vehicle brakes, such that the new velocity v is distributed with a distribution function σ_B depending on the old velocities \hat{v}, \hat{v}_+ .

For the *Acceleration-Interaction* the gain term is given by

$$\hat{G}_A^+(f) = \int \int_{\hat{v} < \hat{v}_+} |\hat{v} - \hat{v}_+| q(H_A(\hat{v}), \hat{v}; \rho, u) \sigma_A(v; \hat{v}, \hat{v}_+) f(x, \hat{v}) F(x + H_A(\hat{v}), \hat{v}_+) d\hat{v} d\hat{v}_+.$$

The loss term is

$$\hat{L}_A^+(f) = \int_{\hat{v}_+ > v} |v - \hat{v}_+| q(H_A(v), \hat{v}_+; \rho, u) f(x, v) F(x + H_A(v), \hat{v}_+) d\hat{v}_+.$$

Thus, again the new velocity is distributed according to σ_A depending on the old velocities. Finally, a relaxation term is introduced, describing a random behaviour of the drivers. It is given by

$$\hat{G}_S(f) = \nu(\rho, u) \int_0^w \sigma_S(v, \hat{v}) f(x, \hat{v}) d\hat{v}$$

where ν denotes an interaction frequency and $\int_0^\infty \sigma_S(v, \hat{v}) dv = 1$. The loss term is

$$\hat{L}_S(f) = \nu(\rho, u) f(v).$$

Remark: For remarks on this Boltzmann/Enskog approach to traffic flow modelling see [11].

In the following these equations are simplified by using appropriate averages. We consider the functions $q(H_X(v), v; \rho, u)$, $X = A, B$ appearing in the above integrals and replace the velocity v in these expressions with the mean velocity u . This means we approximate

$$q(H_A(v), v; \rho, u) \sim q(H_A(u), u; \rho, u) := q_A(\rho, u) = \tilde{\rho} e^{-\tilde{\rho}(T_A - T_B)u}$$

and

$$q(H_B(v), v; \rho, u) \sim q(H_B(u), u; \rho, u) := q_B(\rho, u) = \tilde{\rho}.$$

The probability for braking is approximated using formula (2) and substituting $H_B(v)$ and $q(h, v)$ by $H_B(u)$ and $q(h, u)$, respectively. With $P_B = 1 - P_{ov}$ this gives

$$P_B(\rho, u) = 1 - (1 - \rho H_B(u)) e^{-\frac{\rho H_B(u)}{1 - \rho H_B(u)}} \quad (4)$$

To rewrite the equations in a simpler form we use

$$k = k(\rho, u) = \frac{P_B q_B}{q_A + P_B q_B}$$

and

$$\gamma = \gamma(\rho, u) = \frac{q_A}{1-k} = q_A + P_B q_B.$$

Finally, we define c by

$$\gamma c = \nu$$

and assume for simplicity that c depends on ρ, u through k , that means

$$c = c(k).$$

Using these approximations, Equation (3) is rewritten as

$$\begin{aligned} \partial_t f + v \partial_x f &= C^+(f) \\ &= \gamma [k(G_B^+ - L_B^+)(f) + (1-k)(G_A^+ - L_A^+)(f) + c(G_S - L_S)(f)] \end{aligned}$$

with

$$\begin{aligned} G_B^+(f) &= \int \int_{\hat{v} > \hat{v}_+} |\hat{v} - \hat{v}_+| \sigma_B(v; \hat{v}, \hat{v}_+) f(x, \hat{v}) F(x + H_B(\hat{v}), \hat{v}_+) d\hat{v} d\hat{v}_+ \\ L_B^+(f) &= \int_{\hat{v}_+ < v} |v - \hat{v}_+| f(x, v) F(x + H_B(v), \hat{v}_+) d\hat{v}_+ \\ G_A^+(f) &= \int \int_{\hat{v} < \hat{v}_+} |\hat{v} - \hat{v}_+| \sigma_A(v; \hat{v}, \hat{v}_+) f(x, \hat{v}) F(x + H_A(\hat{v}), \hat{v}_+) d\hat{v} d\hat{v}_+ \\ L_A^+(f) &= \int_{\hat{v}_+ > v} |v - \hat{v}_+| f(x, v) F(x + H_A(v), \hat{v}_+) d\hat{v}_+ \\ G_S(f) &= \int_0^w \sigma_S(v, \hat{v}) f(x, \hat{v}) d\hat{v} \\ L_S(f) &= f(v). \end{aligned}$$

2.3 An example

For the probability distributions σ_A, σ_B we choose the following simple expressions:

$$\sigma_B(v, \hat{v}, \hat{v}_+) = \frac{1}{\hat{v} - \hat{v}_+} \chi_{[\hat{v}_+, \hat{v}]}(v) \quad (5)$$

and

$$\sigma_A(v, \hat{v}, \hat{v}_+) = \frac{1}{\hat{v}_+ - \hat{v}} \chi_{[\hat{v}, \hat{v}_+]}(v). \quad (6)$$

This means we have an equidistribution of the new velocities between the velocity of the car and the velocity of its leading car. Finally,

$$\sigma_S(v, \hat{v}) = \frac{1}{w}. \quad (7)$$

3 Stationary Distributions and Multivalued Fundamental Diagrams

In this section we investigate the stationary homogeneous equations and determine the multivalued fundamental diagrams.

3.1 The general case

We consider the local interaction operator:

$$C(f) = \gamma [k(G_B - L_B)(f) + (1 - k)(G_A - L_A)(f) + c(G_S - L_S)(f)]$$

with $f = \rho F$. The gain and loss terms G_B, L_B , etc. are defined in the same way as G_B^+, L_B^+ , etc., however, $x + H_X(v), X = A, B$ is substituted by x , wherever it appears. The homogeneous stationary equation is

$$C(f) = 0.$$

We assume that for fixed ρ and k there is a unique solution

$$f = f^e = \rho F^e(k, v)$$

of this equation. This is true for the example stated above.

For fixed k the mean value of F^e is

$$u^e(k) = \int_0^w v F^e(k, v) dv.$$

The function u^e is uniquely determined due to the above assumption as a function of k . The fundamental diagram (density-velocity relationship) is then given as the solution u of the equation

$$u = u^e(k(\rho, u))$$

for fixed ρ . If there is a unique solution u we obtain a well defined relation for equilibrium velocity and density, the fundamental diagram. However, in general this equation will have a multitude of different solutions u , even infinitely many. Plotting a dependence of this solution on the density one obtains in the general case a two-dimensional region in the density-velocity plane, where the solutions are located.

3.2 The example

First we determine the stationary solutions $F^e(k)$ for a fixed value of the parameter k . Substituting the explicit expressions (5) – (7) for $\sigma_X, X = A, B, S$

one obtains:

$$\begin{aligned}
G_B(f) &= G_A(f) = \rho \int_0^v F(\hat{v}) d\hat{v} \int_v^w F(\hat{v}) d\hat{v} \\
L_B(f) &= \rho F(v) \left[v \int_0^v F(\hat{v}) d\hat{v} - \int_0^v \hat{v} F(\hat{v}) d\hat{v} \right] \\
L_A(f) &= \rho F(v) \left[\int_v^w \hat{v} F(\hat{v}) d\hat{v} - v \int_v^w F(\hat{v}) d\hat{v} \right] \\
G_S(f) &= \frac{\rho}{w} \\
L_S(f) &= f.
\end{aligned}$$

Defining $\mathcal{F} : [0, w] \rightarrow [0, 1]$ by $\mathcal{F}(v) = \int_0^v F(\hat{v}) d\hat{v}$ and denoting the inverse function with $v(p)$ a straightforward computation shows that the integral equation $C(f) = 0$ is equivalent to the following boundary value problem for $v(p)$:

$$v'' = v' \frac{3p + k - 2}{p(1-p) + \frac{c}{w}}, \quad v(0) = 0, \quad v(1) = w. \quad (8)$$

Using

$$h(p) = \frac{k - p}{(q - (p - \frac{1}{2}))^{\frac{1}{2}+r} (q + (p - \frac{1}{2}))^{\frac{1}{2}-r}}$$

with

$$q = \sqrt{\frac{c}{w} + \frac{1}{4}}, \quad r = \frac{2k - 1}{4q}$$

the solution of (8) is explicitly given as

$$v(p) = w \frac{h(p) - h(0)}{h(1) - h(0)}.$$

A parameter representation of the unique stationary solutions $F = F^e(k, v)$ is for fixed k given as

$$F^e(k, v(p)) = \frac{1}{v'(p)}.$$

The mean velocity $u^e(k)$ of $F^e(k)$ is given by

$$u^e(k) = \int_0^w v F^e(k, v) dv = \int_0^1 v(\bar{p}) d\bar{p} = w \frac{H(1) - H(0) - h(0)}{h(1) - h(0)}$$

with

$$H(p) = \int_0^p h(\tilde{p}) d\tilde{p} = (q - (p - \frac{1}{2}))^{\frac{1}{2}-r} (q + (p - \frac{1}{2}))^{\frac{1}{2}+r}.$$

The multivalued fundamental diagrams are then obtained as the solutions of the equation $u = u^e(k(\rho, u))$ for fixed ρ . A numerical investigation of this nonlinear equation is given in the last section.

4 Derivation of Macroscopic Models

In this section macroscopic equations for density and mean velocity are derived following the procedure in [13].

4.1 Balance Equations

Multiplying the inhomogeneous kinetic equation (3) with 1 and v and integrating it with respect to v one obtains the following set of balance equations:

$$\begin{aligned} \partial_t \rho + \partial_x(\rho u) &= 0 \\ \partial_t(\rho u) + \partial_x(P + \rho u^2) + E &= S \end{aligned} \tag{9}$$

with the 'traffic pressure'

$$P = \int_0^w (v - u)^2 f dv, \tag{10}$$

the Enskog flux term

$$E = \int_0^w v[C(f)(x, v, t) - C^+(f)(x, v, t)] dv, \tag{11}$$

and the source term

$$S = \int_0^w vC(f)(x, v, t) dv. \tag{12}$$

To obtain closed equations for ρ and u one has to specify the dependence of P , E and S on ρ and u .

4.2 Closure Relations

We use the ansatz $f^{ex} = f^{ex}(\rho, u) = f^{ex}(\rho, u, v)$ for the distribution function to approximate the true distribution f and to close the equations. Let the function F^{ex} be defined by

$$f^{ex} = \rho F^{ex}.$$

We require that $F^{ex}(\rho, u)$ fulfills two properties, namely, having density

$$1 = \int F^{ex}(\rho, u, v) dv \quad (13)$$

and mean value

$$u = \int v F^{ex}(\rho, u, v) dv. \quad (14)$$

Note that the equilibrium distribution $F^e(k(\rho, u))$ has a mean value $u^e(k(\rho, u))$ and does not necessarily fulfill the above requirement. We construct F^{ex} using the one parameter family $F^e(k)$ and choosing a suitable value for k . The following simple ansatz for F^{ex} fulfills conditions (13), (14):

$$F^{ex}(u) = F^e(k^e(u)),$$

where $F^e = F^e(k, v)$ is the uniquely defined function from Section 3 and $k^e = k^e(u)$ is the inverse function to u^e , i.e.

$$u^e(k^e(u)) = u.$$

k^e is well defined, if we assume that $u^e(k)$ is strictly monotone decreasing in k . We note that for this definition of $f^{ex}(\rho, u)$ one obtains a positive function f^{ex} for all values of v .

Equation (9) is now closed by approximating the traffic pressure P in (10) with

$$P = \int_0^w (v - u)^2 f dv \sim \int_0^w (v - u)^2 f^{ex}(\rho, u, v) dv = P^{ex}(\rho, u).$$

Moreover, the Enskog term E is approximated by linearizing expression (11) for E in H and substituting $f^{ex}(\rho, u)$ for f . One obtains

$$E \sim c^{ex}(\rho, u) \partial_x u,$$

where $c^{ex}(\rho, u)$ is defined by

$$c^{ex} = -I(f^{ex}, \partial_u F^{ex}).$$

with

$$I(f, g) = I_B(f, g) + I_A(f, g)$$

and

$$I_B(f, g) = \gamma k \int \int_{\hat{v} > \hat{v}_+} |\hat{v} - \hat{v}_+| H_B(\hat{v}) f(\hat{v}) g(\hat{v}_+) \left[\int_0^w v \sigma_B(v, \hat{v}, \hat{v}_+) dv - \hat{v} \right] d\hat{v}_+ d\hat{v}$$

and

$$I_A(f, g) = \gamma(1-k) \int \int_{\hat{v} < \hat{v}_+} |\hat{v} - \hat{v}_+| H_A(\hat{v}) f(\hat{v}) g(\hat{v}_+) \left[\int_0^w v \sigma_A(v, \hat{v}, \hat{v}_+) dv - \hat{v} \right] d\hat{v}_+ d\hat{v}.$$

To compute c^{ex} we use

$$\partial_u F^{ex}(u) = \frac{\partial_k F^e(k^e(u))}{\partial_k u^e(k^e(u))}.$$

Finally, the source term S has to be approximated:

$$S \sim S^{ex}(\rho, u) = \int_0^w v C(f^{ex}) dv.$$

One obtains macroscopic equations of the form

$$\begin{aligned} \partial_t \rho + \partial_x(\rho u) &= 0 \\ \partial_t(\rho u) + \partial_x(P^{ex}(\rho, u) + \rho u^2) + c^{ex}(\rho, u) \partial_x u &= S^{ex}(\rho, u). \end{aligned}$$

4.3 The example

In case of our example the above expressions can be simplified. A short computation shows that for any distribution function f

$$S = \gamma \left(\left(\frac{1}{2} - k \right) P + c\rho \left(\frac{w}{2} - u \right) \right). \quad (15)$$

Using the distribution function $F^e(k)$ the above expression is equal to 0 for arbitrary k . Choosing $k = k^e = k^e(u)$ we get

$$P^{ex}(\rho, u) = \rho c(k^e(u)) \frac{\frac{w}{2} - u}{k^e(u) - \frac{1}{2}}.$$

To compute S^{ex} we use (15) and substitute P^{ex} found above. We obtain

$$S^{ex}(\rho, u) = \gamma \rho \left(\frac{w}{2} - u \right) \left(c(k) - c(k^e(u)) \frac{\frac{1}{2} - k}{\frac{1}{2} - k^e(u)} \right).$$

c^{ex} is computed as described above using the special form of F^e .

5 Numerical Investigations

In this section we investigate the example described in the text. The mean values of the stationary solutions of the homogeneous kinetic equation are discussed together with the resulting macroscopic equations. For the numerical simulations we choose $w = 1$ and $H_0 = 1$. As described above we use different reaction times to describe the drivers' behaviour in different flow situations. Smaller reaction times and smaller distances to the leading cars are associated to higher velocities. In particular, we choose

$$T_B(\rho, u) = 3 + \frac{10}{\pi} \left(\frac{\pi}{2} + \arctan \left(50 \left[\frac{1}{3} + \rho^2 - 2u \right] \right) \right)$$

$T_B(\rho, u)$ is shown in Figure 1 in the admissible range of values (ρ, u) .

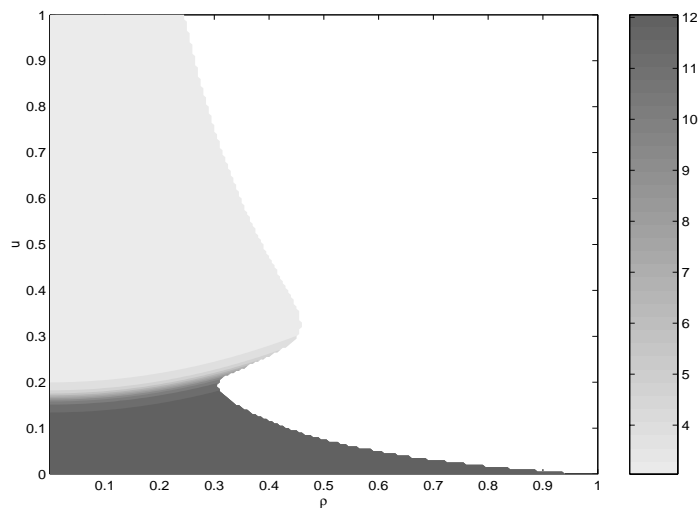


Figure 1: T_B -distribution in the (ρ, u) -plane

For the computations we set $T_A = 2T_B$ and choose c as

$$c(k) = 0.1 k^2 (1 - k)^2.$$

The resulting $P_{ov}(\rho, u)$ is plotted in Figure 2.

Moreover, the results found for the nonlinear equation $u = u^e(k(\rho, u))$ are: There are values ρ_1 and ρ_2 such that for $\rho < \rho_1$ we have only one solution, $u_e^1(\rho)$. For $\rho_1 < \rho < \rho_2$ three solutions $u_e^1(\rho)$, $u_e^2(\rho)$ and $\bar{u}(\rho)$ exist. For the region $\rho > \rho_2$ again only one solution $u_e^2(\rho)$ exists. Figure 3 shows the associated multivalued fundamental diagram.

Finally, the macroscopic equations are investigated for a bottleneck situation. Figures 4 and 5 show the density and flux for a three lane highway with a reduction of lanes from 3 to 2 at $x = 0$. One clearly observes large changes in density ρ and flux $q = \rho u$ in the backwards travelling traffic jam which might be interpreted as stop and go behaviour.

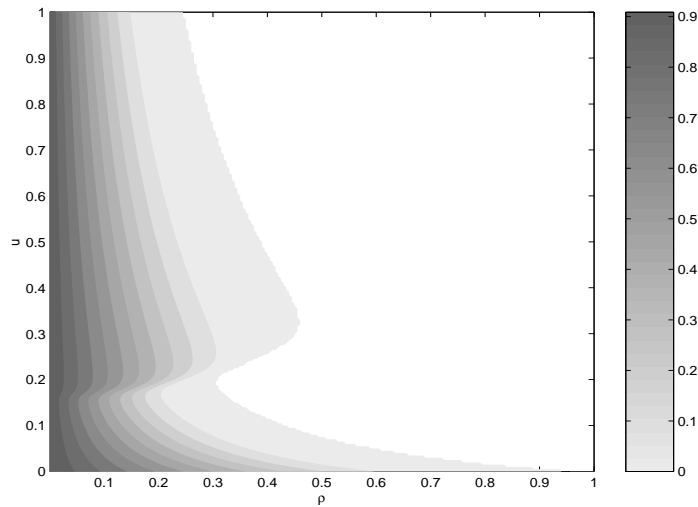


Figure 2: P_{ov} -distribution

Summary

- Multivalued fundamental diagrams are obtained from kinetic equations which match – at least qualitatively – to experimental observations as observed in [9, 10].
- Macroscopic traffic flow models are derived from the kinetic equation.
- These models are able to show stop and go patterns for highway traffic with a bottleneck.

Acknowledgments

The present work has been supported by Deutsche Forschungsgemeinschaft (DFG), KL 1105/5 and the EC network 'HYKE'.

References

- [1] A. AW, *Modèles hyperboliques de trafic automobile*, PhD thesis, Nice, 2001.
- [2] A. AW AND M. RASCLE, *Resurrection of second order models of traffic flow?*, to appear in SIAM J. Appl. Math.
- [3] C. DAGANZO, *Requiem for second order fluid approximations of traffic flow*, Transportation Research B, 29B (1995), pp. 277–286.
- [4] J. GREENBERG, *Extension and amplification of the Aw-Rascle model*, SIAP, 43 (to appear).

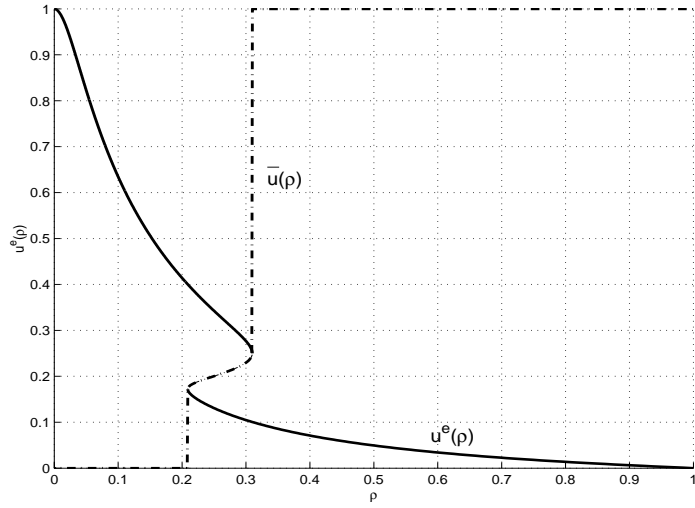


Figure 3: Fundamental diagram.

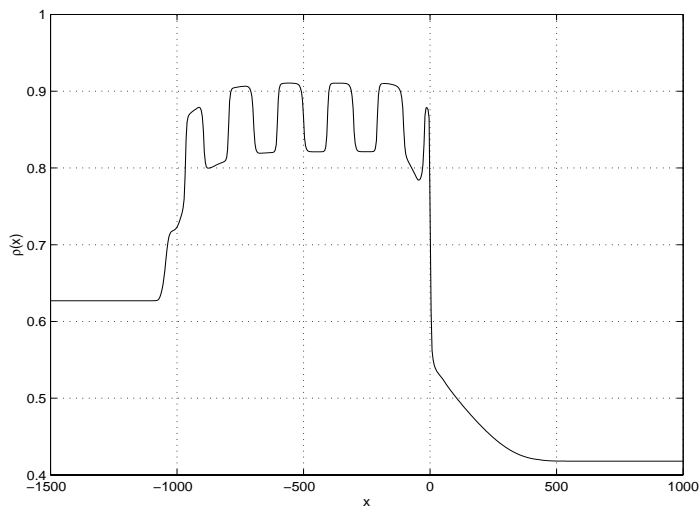


Figure 4: Stop and go waves - density ρ

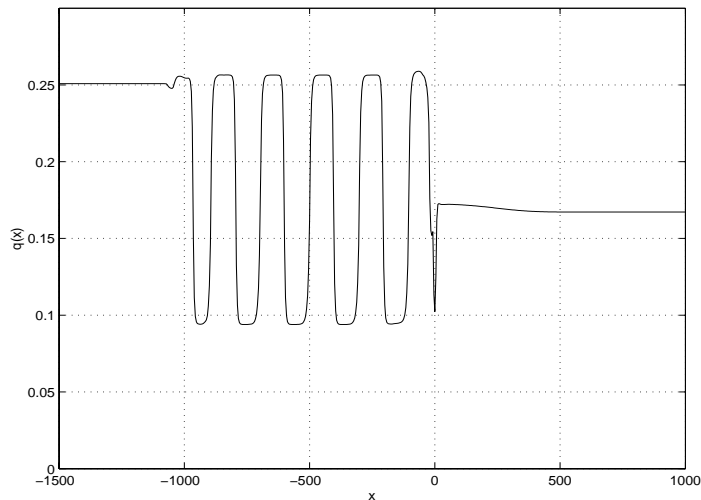


Figure 5: Stop and go waves - flux $q = \rho u$

- [5] J. GREENBERG, A. KLAR, AND M. RASCLE, *Congestion on multilane highways*, preprint.
- [6] D. HELBING, *Gas-kinetic derivation of Navier-Stokes-like traffic equation*, Physical Review E, 53 (1996), pp. 2366–2381.
- [7] R. ILLNER, A. KLAR, AND T. MATERNE, *Vlasov-fokker-planck models for multilane traffic flow*, preprint.
- [8] B. KERNER, *Experimental features of self-organization in traffic flow*, Physical Review Letters, 81 (1998), p. 3797.
- [9] ———, *Congested traffic flow*, Transp. Res. Rec., 1678 (1999), p. 160.
- [10] ———, *Experimental features of the emergence of moving jams in free traffic flow*, J. Phys. A, 33 (2000), p. 221.
- [11] A. KLAR AND R. WEGENER, *Enskog-like kinetic models for vehicular traffic*, J. Stat. Phys., 87 (1997), pp. 91–114.
- [12] ———, *A hierarchy of models for multilane vehicular traffic I: Modeling*, SIAM J. Appl. Math., 59 (1998), pp. 983–1001.
- [13] ———, *Kinetic derivation of macroscopic anticipation models for vehicular traffic*, SIAM J. Appl. Math., 60 (2000), pp. 1749–1766.
- [14] A. NELSON, P. AND SOPASAKIS, *The prigogine-herman kinetic model predicts widely scattered traffic flow data at high concentrations*, Transportation Research, (to appear).
- [15] P. NELSON, *A kinetic model of vehicular traffic and its associated bimodal equilibrium solutions*, Transport Theory and Statistical Physics, 24 (1995), pp. 383–408.

- [16] S. PAVERI-FONTANA, *On Boltzmann like treatments for traffic flow*, Transportation Research, 9 (1975), pp. 225–235.
- [17] H. PAYNE, *FREFLO: A macroscopic simulation model of freeway traffic*, Transportation Research Record, 722 (1979), pp. 68–75.
- [18] I. PRIGOGINE AND R. HERMAN, *Kinetic Theory of Vehicular Traffic*, American Elsevier Publishing Co., New York, 1971.
- [19] G. WHITHAM, *Linear and Nonlinear Waves*, Wiley, New York, 1974.

Bisher erschienene Berichte des Fraunhofer ITWM

Die PDF-Files der folgenden Berichte
finden Sie unter:
www.itwm.fhg.de/zentral/berichte.html

1. D. Hietel, K. Steiner, J. Struckmeier
**A Finite - Volume Particle Method for
Compressible Flows**

We derive a new class of particle methods for conservation laws, which are based on numerical flux functions to model the interactions between moving particles. The derivation is similar to that of classical Finite-Volume methods; except that the fixed grid structure in the Finite-Volume method is substituted by so-called mass packets of particles. We give some numerical results on a shock wave solution for Burgers equation as well as the well-known one-dimensional shock tube problem. (19 S., 1998)

2. M. Feldmann, S. Seibold
**Damage Diagnosis of Rotors: Application
of Hilbert Transform and Multi-Hypothesis
Testing**

In this paper, a combined approach to damage diagnosis of rotors is proposed. The intention is to employ signal-based as well as model-based procedures for an improved detection of size and location of the damage. In a first step, Hilbert transform signal processing techniques allow for a computation of the signal envelope and the instantaneous frequency, so that various types of non-linearities due to a damage may be identified and classified based on measured response data. In a second step, a multi-hypothesis bank of Kalman Filters is employed for the detection of the size and location of the damage based on the information of the type of damage provided by the results of the Hilbert transform.

Keywords:

Hilbert transform, damage diagnosis, Kalman filtering, non-linear dynamics
(23 S., 1998)

3. Y. Ben-Haim, S. Seibold
**Robust Reliability of Diagnostic Multi-
Hypothesis Algorithms: Application to
Rotating Machinery**

Damage diagnosis based on a bank of Kalman filters, each one conditioned on a specific hypothesized system condition, is a well recognized and powerful diagnostic tool. This multi-hypothesis approach can be applied to a wide range of damage conditions. In this paper, we will focus on the diagnosis of cracks in rotating machinery. The question we address is: how to optimize the multi-hypothesis algorithm with respect to the uncertainty of the spatial form and location of cracks and their resulting dynamic effects. First, we formulate a measure of the reliability of the diagnostic algorithm, and then we discuss modifications of the diagnostic algorithm for the maximization of the reliability. The reliability of a diagnostic algorithm is measured by the amount of uncertainty consistent with no-failure of the diagnosis. Uncertainty is quantitatively represented with convex models.

Keywords:

Robust reliability, convex models, Kalman filtering, multi-hypothesis diagnosis, rotating machinery, crack diagnosis
(24 S., 1998)

4. F.-Th. Lenters, N. Siedow
**Three-dimensional Radiative Heat Transfer
in Glass Cooling Processes**

For the numerical simulation of 3D radiative heat transfer in glasses and glass melts, practically applicable mathematical methods are needed to handle such problems optimal using workstation class computers. Since the exact solution would require super-computer capabilities we concentrate on approximate solutions with a high degree of accuracy. The following approaches are studied: 3D diffusion approximations and 3D ray-tracing methods. (23 S., 1998)

5. A. Klar, R. Wegener
**A hierarchy of models for multilane
vehicular traffic
Part I: Modeling**

In the present paper multilane models for vehicular traffic are considered. A microscopic multilane model based on reaction thresholds is developed. Based on this model an Enskog like kinetic model is developed. In particular, care is taken to incorporate the correlations between the vehicles. From the kinetic model a fluid dynamic model is derived. The macroscopic coefficients are deduced from the underlying kinetic model. Numerical simulations are presented for all three levels of description in [10]. Moreover, a comparison of the results is given there. (23 S., 1998)

**Part II: Numerical and stochastic
investigations**

In this paper the work presented in [6] is continued. The present paper contains detailed numerical investigations of the models developed there. A numerical method to treat the kinetic equations obtained in [6] are presented and results of the simulations are shown. Moreover, the stochastic correlation model used in [6] is described and investigated in more detail. (17 S., 1998)

6. A. Klar, N. Siedow
**Boundary Layers and Domain Decomposition
for Radiative Heat Transfer and Diffusion
Equations: Applications to Glass Manu-
facturing Processes**

In this paper domain decomposition methods for radiative transfer problems including conductive heat transfer are treated. The paper focuses on semi-transparent materials, like glass, and the associated conditions at the interface between the materials. Using asymptotic analysis we derive conditions for the coupling of the radiative transfer equations and a diffusion approximation. Several test cases are treated and a problem appearing in glass manufacturing processes is computed. The results clearly show the advantages of a domain decomposition approach. Accuracy equivalent to the solution of the global radiative transfer solution is achieved, whereas computation time is strongly reduced. (24 S., 1998)

7. I. Choquet
**Heterogeneous catalysis modelling and
numerical simulation in rarified gas flows
Part I: Coverage locally at equilibrium**

A new approach is proposed to model and simulate numerically heterogeneous catalysis in rarefied gas flows. It is developed to satisfy all together the following points: 1) describe the gas phase at the microscopic scale, as required in rarefied flows, 2) describe the wall at the macroscopic scale, to avoid prohibitive computational costs and consider not only crystalline but also amorphous surfaces, 3) reproduce on average macroscopic laws correlated with experimental results and 4) derive analytic models in a systematic and exact way. The problem is stated in the general framework of a non static flow in the vicinity of a catalytic and non porous surface (without aging). It is shown that the exact and systematic resolution method based on the Laplace transform, introduced previously by the author to model collisions in the gas phase, can be extended to the present problem. The proposed approach is applied to the modelling of the Eley-Rideal and Langmuir-Hinshelwood recombinations, assuming that the coverage is locally at equilibrium. The models are developed considering one atomic species and extended to the general case of several atomic species. Numerical calculations show that the models derived in this way reproduce with accuracy behaviors observed experimentally. (24 S., 1998)

8. J. Ohser, B. Steinbach, C. Lang
Efficient Texture Analysis of Binary Images

A new method of determining some characteristics of binary images is proposed based on a special linear filtering. This technique enables the estimation of the area fraction, the specific line length, and the specific integral of curvature. Furthermore, the specific length of the total projection is obtained, which gives detailed information about the texture of the image. The influence of lateral and directional resolution depending on the size of the applied filter mask is discussed in detail. The technique includes a method of increasing directional resolution for texture analysis while keeping lateral resolution as high as possible. (17 S., 1998)

9. J. Orlik
**Homogenization for viscoelasticity of the
integral type with aging and shrinkage**

A multi-phase composite with periodic distributed inclusions with a smooth boundary is considered in this contribution. The composite component materials are supposed to be linear viscoelastic and aging (of the non-convolution integral type, for which the Laplace transform with respect to time is not effectively applicable) and are subjected to isotropic shrinkage. The free shrinkage deformation can be considered as a fictitious temperature deformation in the behavior law. The procedure presented in this paper proposes a way to determine average (effective homogenized) viscoelastic and shrinkage (temperature) composite properties and the homogenized stress-field from known properties of the

components. This is done by the extension of the asymptotic homogenization technique known for pure elastic non-homogeneous bodies to the non-homogeneous thermo-viscoelasticity of the integral non-convolution type. Up to now, the homogenization theory has not covered viscoelasticity of the integral type. Sanchez-Palencia (1980), Francfort & Suquet (1987) (see [2], [9]) have considered homogenization for viscoelasticity of the differential form and only up to the first derivative order. The integral-modeled viscoelasticity is more general than the differential one and includes almost all known differential models. The homogenization procedure is based on the construction of an asymptotic solution with respect to a period of the composite structure. This reduces the original problem to some auxiliary boundary value problems of elasticity and viscoelasticity on the unit periodic cell, of the same type as the original non-homogeneous problem. The existence and uniqueness results for such problems were obtained for kernels satisfying some constraint conditions. This is done by the extension of the Volterra integral operator theory to the Volterra operators with respect to the time, whose kernels are space linear operators for any fixed time variables. Some ideas of such approach were proposed in [11] and [12], where the Volterra operators with kernels depending additionally on parameter were considered. This manuscript delivers results of the same nature for the case of the space-operator kernels. (20 S., 1998)

10. J. Mohring

Helmholtz Resonators with Large Aperture

The lowest resonant frequency of a cavity resonator is usually approximated by the classical Helmholtz formula. However, if the opening is rather large and the front wall is narrow this formula is no longer valid. Here we present a correction which is of third order in the ratio of the diameters of aperture and cavity. In addition to the high accuracy it allows to estimate the damping due to radiation. The result is found by applying the method of matched asymptotic expansions. The correction contains form factors describing the shapes of opening and cavity. They are computed for a number of standard geometries. Results are compared with numerical computations. (21 S., 1998)

11. H. W. Hamacher, A. Schöbel

On Center Cycles in Grid Graphs

Finding "good" cycles in graphs is a problem of great interest in graph theory as well as in locational analysis. We show that the center and median problems are NP hard in general graphs. This result holds both for the variable cardinality case (i.e. all cycles of the graph are considered) and the fixed cardinality case (i.e. only cycles with a given cardinality p are feasible). Hence it is of interest to investigate special cases where the problem is solvable in polynomial time. In grid graphs, the variable cardinality case is, for instance, trivially solvable if the shape of the cycle can be chosen freely. If the shape is fixed to be a rectangle one can analyze rectangles in grid graphs with, in sequence, fixed dimension, fixed cardinality, and variable cardinality. In all cases a complete characterization of the optimal cycles and closed form expressions of the optimal objective values are given, yielding polynomial time algorithms for all cases of center rectangle problems. Finally, it is shown that center cycles can be chosen as

rectangles for small cardinalities such that the center cycle problem in grid graphs is in these cases completely solved. (15 S., 1998)

12. H. W. Hamacher, K.-H. Küfer

Inverse radiation therapy planning - a multiple objective optimisation approach

For some decades radiation therapy has been proved successful in cancer treatment. It is the major task of clinical radiation treatment planning to realize on the one hand a high level dose of radiation in the cancer tissue in order to obtain maximum tumor control. On the other hand it is obvious that it is absolutely necessary to keep in the tissue outside the tumor, particularly in organs at risk, the unavoidable radiation as low as possible. No doubt, these two objectives of treatment planning - high level dose in the tumor, low radiation outside the tumor - have a basically contradictory nature. Therefore, it is no surprise that inverse mathematical models with dose distribution bounds tend to be infeasible in most cases. Thus, there is need for approximations compromising between overdosing the organs at risk and underdosing the target volume.

Differing from the currently used time consuming iterative approach, which measures deviation from an ideal (non-achievable) treatment plan using recursively trial-and-error weights for the organs of interest, we go a new way trying to avoid a priori weight choices and consider the treatment planning problem as a multiple objective linear programming problem: with each organ of interest, target tissue as well as organs at risk, we associate an objective function measuring the maximal deviation from the prescribed doses.

We build up a data base of relatively few efficient solutions representing and approximating the variety of Pareto solutions of the multiple objective linear programming problem. This data base can be easily scanned by physicians looking for an adequate treatment plan with the aid of an appropriate online tool. (14 S., 1999)

13. C. Lang, J. Ohser, R. Hilfer

On the Analysis of Spatial Binary Images

This paper deals with the characterization of microscopically heterogeneous, but macroscopically homogeneous spatial structures. A new method is presented which is strictly based on integral-geometric formulae such as Crofton's intersection formulae and Hadwiger's recursive definition of the Euler number. The corresponding algorithms have clear advantages over other techniques. As an example of application we consider the analysis of spatial digital images produced by means of Computer Assisted Tomography. (20 S., 1999)

14. M. Junk

On the Construction of Discrete Equilibrium Distributions for Kinetic Schemes

A general approach to the construction of discrete equilibrium distributions is presented. Such distribution functions can be used to set up Kinetic Schemes as well as Lattice Boltzmann methods. The general principles are also applied to the construction of Chapman Enskog distributions which are used in Kinetic Schemes for com-

pressible Navier-Stokes equations. (24 S., 1999)

15. M. Junk, S. V. Raghurame Rao

A new discrete velocity method for Navier-Stokes equations

The relation between the Lattice Boltzmann Method, which has recently become popular, and the Kinetic Schemes, which are routinely used in Computational Fluid Dynamics, is explored. A new discrete velocity model for the numerical solution of Navier-Stokes equations for incompressible fluid flow is presented by combining both the approaches. The new scheme can be interpreted as a pseudo-compressibility method and, for a particular choice of parameters, this interpretation carries over to the Lattice Boltzmann Method. (20 S., 1999)

16. H. Neunzert

Mathematics as a Key to Key Technologies

The main part of this paper will consist of examples, how mathematics really helps to solve industrial problems; these examples are taken from our Institute for Industrial Mathematics, from research in the Technomathematics group at my university, but also from ECMI groups and a company called TecMath, which originated 10 years ago from my university group and has already a very successful history. (39 S. (vier PDF-Files), 1999)

17. J. Ohser, K. Sandau

Considerations about the Estimation of the Size Distribution in Wickcell's Corpuscle Problem

Wickcell's corpuscle problem deals with the estimation of the size distribution of a population of particles, all having the same shape, using a lower dimensional sampling probe. This problem was originally formulated for particle systems occurring in life sciences but its solution is of actual and increasing interest in materials science. From a mathematical point of view, Wickcell's problem is an inverse problem where the interesting size distribution is the unknown part of a Volterra equation. The problem is often regarded ill-posed, because the structure of the integrand implies unstable numerical solutions. The accuracy of the numerical solutions is considered here using the condition number, which allows to compare different numerical methods with different (equidistant) class sizes and which indicates, as one result, that a finite section thickness of the probe reduces the numerical problems. Furthermore, the relative error of estimation is computed which can be split into two parts. One part consists of the relative discretization error that increases for increasing class size, and the second part is related to the relative statistical error which increases with decreasing class size. For both parts, upper bounds can be given and the sum of them indicates an optimal class width depending on some specific constants. (18 S., 1999)

18. E. Carrizosa, H. W. Hamacher, R. Klein, S. Nickel

Solving nonconvex planar location problems by finite dominating sets

It is well-known that some of the classical location problems with polyhedral gauges can be solved in polynomial time by finding a finite dominating set, i. e. a finite set of candidates guaranteed to contain at least one optimal location.

In this paper it is first established that this result holds for a much larger class of problems than currently considered in the literature. The model for which this result can be proven includes, for instance, location problems with attraction and repulsion, and location-allocation problems. Next, it is shown that the approximation of general gauges by polyhedral ones in the objective function of our general model can be analyzed with regard to the subsequent error in the optimal objective value. For the approximation problem two different approaches are described, the sandwich procedure and the greedy algorithm. Both of these approaches lead - for fixed epsilon - to polynomial approximation algorithms with accuracy epsilon for solving the general model considered in this paper.

Keywords:

Continuous Location, Polyhedral Gauges, Finite Dominating Sets, Approximation, Sandwich Algorithm, Greedy Algorithm (19 S., 2000)

19. A. Becker

A Review on Image Distortion Measures

Within this paper we review image distortion measures. A distortion measure is a criterion that assigns a "quality number" to an image. We distinguish between mathematical distortion measures and those distortion measures in-cooperating a priori knowledge about the imaging devices (e. g. satellite images), image processing algorithms or the human physiology. We will consider representative examples of different kinds of distortion measures and are going to discuss them.

Keywords:

Distortion measure, human visual system (26 S., 2000)

20. H. W. Hamacher, M. Labbé, S. Nickel, T. Sonneborn

Polyhedral Properties of the Uncapacitated Multiple Allocation Hub Location Problem

We examine the feasibility polyhedron of the uncapacitated hub location problem (UHL) with multiple allocation, which has applications in the fields of air passenger and cargo transportation, telecommunication and postal delivery services. In particular we determine the dimension and derive some classes of facets of this polyhedron. We develop some general rules about lifting facets from the uncapacitated facility location (UFL) for UHL and projecting facets from UHL to UFL. By applying these rules we get a new class of facets for UHL which dominates the inequalities in the original formulation. Thus we get a new formulation of UHL whose constraints are all facet-defining. We show its superior computational performance by benchmarking it on a well known data set.

Keywords:

integer programming, hub location, facility location, valid inequalities, facets, branch and cut (21 S., 2000)

21. H. W. Hamacher, A. Schöbel

Design of Zone Tariff Systems in Public Transportation

Given a public transportation system represented by its stops and direct connections between stops, we consider two problems dealing with the prices for the customers: The fare problem in which subsets of stops are already aggregated to zones and "good" tariffs have to be found in the existing zone system. Closed form solutions for the fare problem are presented for three objective functions. In the zone problem the design of the zones is part of the problem. This problem is NP hard and we therefore propose three heuristics which prove to be very successful in the redesign of one of Germany's transportation systems.

(30 S., 2001)

22. D. Hietel, M. Junk, R. Keck, D. Teleaga:

The Finite-Volume-Particle Method for Conservation Laws

In the Finite-Volume-Particle Method (FVPM), the weak formulation of a hyperbolic conservation law is discretized by restricting it to a discrete set of test functions. In contrast to the usual Finite-Volume approach, the test functions are not taken as characteristic functions of the control volumes in a spatial grid, but are chosen from a partition of unity with smooth and overlapping partition functions (the particles), which can even move along prescribed velocity fields. The information exchange between particles is based on standard numerical flux functions. Geometrical information, similar to the surface area of the cell faces in the Finite-Volume Method and the corresponding normal directions are given as integral quantities of the partition functions.

After a brief derivation of the Finite-Volume-Particle Method, this work focuses on the role of the geometric coefficients in the scheme.

(16 S., 2001)

23. T. Bender, H. Hennes, J. Kalcsics, M. T. Melo, S. Nickel

Location Software and Interface with GIS and Supply Chain Management

The objective of this paper is to bridge the gap between location theory and practice. To meet this objective focus is given to the development of software capable of addressing the different needs of a wide group of users. There is a very active community on location theory encompassing many research fields such as operations research, computer science, mathematics, engineering, geography, economics and marketing. As a result, people working on facility location problems have a very diverse background and also different needs regarding the software to solve these problems. For those interested in non-commercial applications (e. g. students and researchers), the library of location algorithms (LoLA can be of considerable assistance. LoLA contains a collection of efficient algorithms for solving planar, network and discrete facility location problems. In this paper, a detailed description of the functionality of LoLA is presented. In the fields of geography and marketing, for instance, solving facility location problems requires using large amounts of demographic data. Hence, members of these groups (e. g. urban planners and sales managers) often work with geographical information too. To address the specific needs of these users, LoLA was linked to a geo-

graphical information system (GIS) and the details of the combined functionality are described in the paper. Finally, there is a wide group of practitioners who need to solve large problems and require special purpose software with a good data interface. Many of such users can be found, for example, in the area of supply chain management (SCM). Logistics activities involved in strategic SCM include, among others, facility location planning. In this paper, the development of a commercial location software tool is also described. The tool is embedded in the Advanced Planner and Optimizer SCM software developed by SAP AG, Walldorf, Germany. The paper ends with some conclusions and an outlook to future activities.

Keywords:

facility location, software development, geographical information systems, supply chain management. (48 S., 2001)

24. H. W. Hamacher, S. A. Tjandra

Mathematical Modelling of Evacuation Problems: A State of Art

This paper details models and algorithms which can be applied to evacuation problems. While it concentrates on building evacuation many of the results are applicable also to regional evacuation. All models consider the time as main parameter, where the travel time between components of the building is part of the input and the overall evacuation time is the output. The paper distinguishes between macroscopic and microscopic evacuation models both of which are able to capture the evacuees' movement over time.

Macroscopic models are mainly used to produce good lower bounds for the evacuation time and do not consider any individual behavior during the emergency situation. These bounds can be used to analyze existing buildings or help in the design phase of planning a building. Macroscopic approaches which are based on dynamic network flow models (minimum cost dynamic flow, maximum dynamic flow, universal maximum flow, quickest path and quickest flow) are described. A special feature of the presented approach is the fact, that travel times of evacuees are not restricted to be constant, but may be density dependent. Using multicriteria optimization priority regions and blockage due to fire or smoke may be considered. It is shown how the modelling can be done using time parameter either as discrete or continuous parameter.

Microscopic models are able to model the individual evacuee's characteristics and the interaction among evacuees which influence their movement. Due to the corresponding huge amount of data one uses simulation approaches. Some probabilistic laws for individual evacuee's movement are presented. Moreover ideas to model the evacuee's movement using cellular automata (CA) and resulting software are presented.

In this paper we will focus on macroscopic models and only summarize some of the results of the microscopic approach. While most of the results are applicable to general evacuation situations, we concentrate on building evacuation.

(44 S., 2001)

25. J. Kuhnert, S. Tiwari

Grid free method for solving the Poisson equation

A Grid free method for solving the Poisson equation is presented. This is an iterative method. The method is based on the weighted least squares approximation in which the Poisson equation is enforced to be satisfied in every iterations. The boundary conditions can also be enforced in the iteration process. This is a local approximation procedure. The Dirichlet, Neumann and mixed boundary value problems on a unit square are presented and the analytical solutions are compared with the exact solutions. Both solutions matched perfectly.

Keywords:

Poisson equation, Least squares method, Grid free method (19 S., 2001)

26. T. Götz, H. Rave, D. Reinel-Bitzer, K. Steiner, H. Tiemeier

Simulation of the fiber spinning process

To simulate the influence of process parameters to the melt spinning process a fiber model is used and coupled with CFD calculations of the quench air flow. In the fiber model energy, momentum and mass balance are solved for the polymer mass flow. To calculate the quench air the Lattice Boltzmann method is used. Simulations and experiments for different process parameters and hole configurations are compared and show a good agreement.

Keywords:

Melt spinning, fiber model, Lattice Boltzmann, CFD (19 S., 2001)

27. A. Zemitis

On interaction of a liquid film with an obstacle

In this paper mathematical models for liquid films generated by impinging jets are discussed. Attention is stressed to the interaction of the liquid film with some obstacle. S. G. Taylor [Proc. R. Soc. London Ser. A 253, 313 (1959)] found that the liquid film generated by impinging jets is very sensitive to properties of the wire which was used as an obstacle. The aim of this presentation is to propose a modification of the Taylor's model, which allows to simulate the film shape in cases, when the angle between jets is different from 180°. Numerical results obtained by discussed models give two different shapes of the liquid film similar as in Taylors experiments. These two shapes depend on the regime: either droplets are produced close to the obstacle or not. The difference between two regimes becomes larger if the angle between jets decreases. Existence of such two regimes can be very essential for some applications of impinging jets, if the generated liquid film can have a contact with obstacles.

Keywords:

impinging jets, liquid film, models, numerical solution, shape (22 S., 2001)

28. I. Ginzburg, K. Steiner

Free surface lattice-Boltzmann method to model the filling of expanding cavities by Bingham Fluids

The filling process of viscoplastic metal alloys and plastics in expanding cavities is modelled using the lattice Boltzmann method in two and three dimensions. These models combine the regularized Bingham model for viscoplastic with a free-interface algorithm. The latter is based on a modified immiscible lattice Boltzmann model in which one species is the fluid and the other one is considered as vacuum. The boundary conditions at the curved liquid-vacuum interface are met without any geometrical front reconstruction from a first-order Chapman-Enskog expansion. The numerical results obtained with these models are found in good agreement with available theoretical and numerical analysis.

Keywords:

Generalized LBE, free-surface phenomena, interface boundary conditions, filling processes, Bingham viscoplastic model, regularized models (22 S., 2001)

29. H. Neunzert

»Denn nichts ist für den Menschen als Menschen etwas wert, was er nicht mit Leidenschaft tun kann«

Vortrag anlässlich der Verleihung des Akademiepreises des Landes Rheinland-Pfalz am 21.11.2001

Was macht einen guten Hochschullehrer aus? Auf diese Frage gibt es sicher viele verschiedene, fachbezogene Antworten, aber auch ein paar allgemeine Gesichtspunkte: es bedarf der »Leidenschaft« für die Forschung (Max Weber), aus der dann auch die Begeisterung für die Lehre erwächst. Forschung und Lehre gehören zusammen, um die Wissenschaft als lebendiges Tun vermitteln zu können. Der Vortrag gibt Beispiele dafür, wie in angewandter Mathematik Forschungsaufgaben aus praktischen Alltagsproblemstellungen erwachsen, die in die Lehre auf verschiedenen Stufen (Gymnasium bis Graduiertenkolleg) einfließen; er leitet damit auch zu einem aktuellen Forschungsgebiet, der Mehrskalalanalyse mit ihren vielfältigen Anwendungen in Bildverarbeitung, Materialentwicklung und Strömungsmechanik über, was aber nur kurz gestreift wird. Mathematik erscheint hier als eine moderne Schlüsseltechnologie, die aber auch enge Beziehungen zu den Geistes- und Sozialwissenschaften hat.

Keywords:

Lehre, Forschung, angewandte Mathematik, Mehrskalalanalyse, Strömungsmechanik (18 S., 2001)

30. J. Kuhnert, S. Tiwari

Finite pointset method based on the projection method for simulations of the incompressible Navier-Stokes equations

A Lagrangian particle scheme is applied to the projection method for the incompressible Navier-Stokes equations. The approximation of spatial derivatives is obtained by the weighted least squares method. The pressure Poisson equation is solved by a local iterative procedure with the help of the least squares method. Numerical tests are performed for two dimensional cases. The Couette flow, Poiseuille flow, decaying shear flow and the driven cavity

flow are presented. The numerical solutions are obtained for stationary as well as instationary cases and are compared with the analytical solutions for channel flows. Finally, the driven cavity in a unit square is considered and the stationary solution obtained from this scheme is compared with that from the finite element method.

Keywords:

Incompressible Navier-Stokes equations, Meshfree method, Projection method, Particle scheme, Least squares approximation
AMS subject classification:
76D05, 76M28
(25 S., 2001)

31. R. Korn, M. Krekel

Optimal Portfolios with Fixed Consumption or Income Streams

We consider some portfolio optimisation problems where either the investor has a desire for an a priori specified consumption stream or/and follows a deterministic pay in scheme while also trying to maximize expected utility from final wealth. We derive explicit closed form solutions for continuous and discrete monetary streams. The mathematical method used is classical stochastic control theory.

Keywords:

Portfolio optimisation, stochastic control, HJB equation, discretisation of control problems.
(23 S., 2002)

32. M. Krekel

Optimal portfolios with a loan dependent credit spread

If an investor borrows money he generally has to pay higher interest rates than he would have received, if he had put his funds on a savings account. The classical model of continuous time portfolio optimisation ignores this effect. Since there is obviously a connection between the default probability and the total percentage of wealth, which the investor is in debt, we study portfolio optimisation with a control dependent interest rate. Assuming a logarithmic and a power utility function, respectively, we prove explicit formulae of the optimal control.

Keywords:

Portfolio optimisation, stochastic control, HJB equation, credit spread, log utility, power utility, non-linear wealth dynamics
(25 S., 2002)

33. J. Ohser, W. Nagel, K. Schladitz

The Euler number of discretized sets - on the choice of adjacency in homogeneous lattices

Two approaches for determining the Euler-Poincaré characteristic of a set observed on lattice points are considered in the context of image analysis { the integral geometric and the polyhedral approach. Information about the set is assumed to be available on lattice points only. In order to retain properties of the Euler number and to provide a good approximation of the true Euler number of the original set in the Euclidean space, the appropriate choice of adjacency in the lattice for the set and its background is crucial. Adjacencies are defined using tessellations of the whole space into polyhedrons. In \mathbb{R}^3 , two new 14 adjacencies are introduced additionally to the

well known 6 and 26 adjacencies. For the Euler number of a set and its complement, a consistency relation holds. Each of the pairs of adjacencies (14:1; 14:1), (14:2; 14:2), (6; 26), and (26; 6) is shown to be a pair of complementary adjacencies with respect to this relation. That is, the approximations of the Euler numbers are consistent if the set and its background (complement) are equipped with this pair of adjacencies. Furthermore, sufficient conditions for the correctness of the approximations of the Euler number are given. The analysis of selected microstructures and a simulation study illustrate how the estimated Euler number depends on the chosen adjacency. It also shows that there is not a uniquely best pair of adjacencies with respect to the estimation of the Euler number of a set in Euclidean space.

Keywords: image analysis, Euler number, neighborhood relationships, cuboidal lattice
(32 S., 2002)

Keywords: traffic flow, macroscopic equations, kinetic derivation, multivalued fundamental diagram, stop and go waves, phase transitions
(25 S., 2002)

34. I. Ginzburg, K. Steiner

Lattice Boltzmann Model for Free-Surface flow and Its Application to Filling Process in Casting

A generalized lattice Boltzmann model to simulate free-surface is constructed in both two and three dimensions. The proposed model satisfies the interfacial boundary conditions accurately. A distinctive feature of the model is that the collision processes is carried out only on the points occupied partially or fully by the fluid. To maintain a sharp interfacial front, the method includes an anti-diffusion algorithm. The unknown distribution functions at the interfacial region are constructed according to the first order Chapman-Enskog analysis. The interfacial boundary conditions are satisfied exactly by the coefficients in the Chapman-Enskog expansion. The distribution functions are naturally expressed in the local interfacial coordinates. The macroscopic quantities at the interface are extracted from the least-square solutions of a locally linearized system obtained from the known distribution functions. The proposed method does not require any geometric front construction and is robust for any interfacial topology. Simulation results of realistic filling process are presented: rectangular cavity in two dimensions and Hammer box, Campbell box, Sheffield box, and Motorblock in three dimensions. To enhance the stability at high Reynolds numbers, various upwind-type schemes are developed. Free-slip and no-slip boundary conditions are also discussed.

Keywords: Lattice Boltzmann models; free-surface phenomena; interface boundary conditions; filling processes; injection molding; volume of fluid method; interface boundary conditions; advection-schemes; upwind-schemes
(54 S., 2002)

35. M. Günther, A. Klar, T. Materne, R. Wegener

Multivalued fundamental diagrams and stop and go waves for continuum traffic equations

In the present paper a kinetic model for vehicular traffic leading to multivalued fundamental diagrams is developed and investigated in detail. For this model phase transitions can appear depending on the local density and velocity of the flow. A derivation of associated macroscopic traffic equations from the kinetic equation is given. Moreover, numerical experiments show the appearance of stop and go waves for highway traffic with a bottleneck.